Title

Tidal response variation and recovery following the Wenchuan earthquake from water level data of multiple wells in the nearfield

Authors

Lai, Guijuan
Ge, Hongkui
Xue, Lian
et al.

Publication Date

2013-09-06

Peer reviewed

Tectonophysics 619–620 (2014) 115–122

Contents lists available at ScienceDirect

Tectonophysics

journal homepage: www.elsevier.com/locate/tecto

Tidal response variation and recovery following the Wenchuan earthquake from water level data of multiple wells in the nearfield

Guijuan Lai [a,c], Hongkui Ge [b], Lian Xue [c], Emily E. Brodsky [c], Fuqiong Huang [d], Weilai Wang [a,e,*]

[a] Key Laboratory of Seismic Observation and Geophysical Imaging, Institute of Geophysics, China Earthquake Administration, Beijing 100081, China
[b] Unconventional Natural Gas Institute, China University of Petroleum, Beijing 102249, China
[c] Department of Earth and Planetary Sciences, University of California, Santa Cruz, CA 95060, USA
[d] China Earthquake Networks Center, Beijing 100045, China
[e] Institute of Geophysics, China Earthquake Administration, Beijing 100081, China

ARTICLE INFO

Article history:
Received 20 March 2013
Received in revised form 21 August 2013
Accepted 29 August 2013
Available online 6 September 2013

Keywords:
Wenchuan earthquake
Permeability variation
Recovery time
Coseismic water level changes
Tidal response

ABSTRACT

An important dataset to emerge from the Wenchuan earthquake Fault Scientific Drilling project is direct measurement of the permeability evolution of a fault zone. In order to provide context for this new observation, we examined the evolution of tidal responses in the nearfield region (within ~1.5 fault lengths) at the time of the mainshock. Previous work has shown that seismic waves can increase permeability in the farfield, but their effects in the nearfield are more difficult to discern. Close to an earthquake, hydrogeological responses are generally a combination of static and dynamic stresses. In this work, we examine the well water level data in the region of the large M_w 7.9 Wenchuan earthquake and use the phase shift of tidal responses as a proxy for the permeability variations over time. We then compare the results with the coseismic water level pattern in order to separate out the dynamic and static effects. The coseismic water level pattern for observed steps coincident with the Wenchuan mainshock mainly tracks the expected static stress field. However, most of the wells that have resolvable tidal responses show permeability enhancement after this large earthquake regardless of whether the coseismic response for the well water level is increasing or decreasing, indicating permeability enhancement is a distinct process from static poroelastic strain.

1. Introduction

It has been reported for a long time that large earthquakes can cause various hydrological responses, such as the variations in groundwater level (Akita and Matsumoto, 2001; Chia et al., 2008; Huang et al., 2004; S.H. Lee et al., 2012; T.-P. Lee et al., 2012; Liu et al., 1989; Niwa et al., 2012; Roeloffs, 1996; Sil, 2006), springs and stream discharge (Manga, 2001; Manga and Rowland, 2009; Manga et al., 2003; Mohr et al., 2012; Montgomery and Manga, 2003; Wang et al., 2004). Among them, changes in well water levels are the most commonly reported phenomenon.

Abrupt changes in well water levels in the nearfield (within 1–2 fault lengths) are often explained by the static poroelastic strain of aquifers caused by earthquakes (Akita and Matsumoto, 2004; Matsumoto and Roeloffs, 2003; Roeloffs and Bredehoeft, 1985; Shi et al., 2012; Shibata et al., 2010; Wakita, 1975; Wang and Chia, 2008; Zhang and Huang, 2011). In the intermediate and farfield (many fault lengths), the static poroelastic strains from displacement during earthquakes are small and can fail to explain the sign of the sustained variations in water levels (Manga et al., 2003). Brodsky et al. (2003) proposed a new model for coseismic pore pressure steps in the farfield, in which the temporary barriers from the groundwater flow are removed by more rapid flow caused by seismic waves and thus the permeability is enhanced. This hypothesis was supported by subsequent observations of permeability enhancement in the farfield (Elkhoury et al., 2006; Geballe et al., 2011; Manga et al., 2012; Wang et al., 2009). Xue et al. (2013) found a similar phenomenon in the deep borehole at WFSD-1 (Wenchuan earthquake Fault Scientific Drilling) where post-mainshock healing is interrupted by permeability increases associated with regional and teleseismic earthquakes. The permeability enhancement hypothesis therefore appears to be useful for farfield datasets.

As the datasets of permeability changes increase, a persistent question is the relative importance of the poroelastic and dynamic stresses in controlling the permeability changes in the nearfield where the static and dynamic stress fields are more difficult to disentangle. Here we use the exemplary digital data of the Groundwater Monitoring Network (GMN) of water wells in the region of the Wenchuan earthquake to examine this question.

The great M_w 7.9 Wenchuan earthquake on May 12, 2008 caused widespread water level changes both on the Chinese mainland and in the Taiwan region (e.g. S.H. Lee et al., 2012; T.-P. Lee et al., 2012; Yang et al., 2008). Huang (2008) studied the coseismic water level steps on

* Corresponding author at: No. 5 Minzu Daxue Nan Rd., Haidian District, Beijing 100081, China.
E-mail address: cathy_313@163.com (W. Wang).

0040-1951/$ – see front matter © 2013 Elsevier B.V. All rights reserved.
http://dx.doi.org/10.1016/j.tecto.2013.08.039

the Chinese mainland in response to this earthquake, and proposed that for confined and consolidated aquifers, water level changes reflect the change in the in-situ borehole strain. Zhang and Huang (2011) found that the poroelastic theory can be used to explain the coseismic water level changes within 1.5 fault lengths. Shi et al. (2012) revisited this problem and concluded that within 500 km, the sign of the coseismic water level changes can match the static stress field predicted from a dislocation model, though the magnitudes may be inconsistent for some wells. In this paper, we examine the underground water level data in the region of this large earthquake, use the phase shift of tidal responses as a proxy for the permeability variations over time for the wells that have resolvable tidal responses, and compare the results to both the predicted static stress field and the coseismic water level step pattern. We attempt to study the permeability variation and recovery time following this large earthquake in the nearfield, which is significant for understanding the physical origin of permeability variation and recovery.

2. Data

The digital transformation of the Groundwater Monitoring Network (GMN) in China was completed by the end of 2007. The water levels in wells are measured by the LN-3 digital recorders, and the sampling interval is 1 min (The Monitoring and Forecasting Department of China Earthquake Administration, 2007). The great M_w 7.9 Wenchuan earthquake happened on May 12, 2008, so we were able to collate data from the GMN of the China Earthquake Networks Center from 2007 to 2009 in the nearfield, which we define as within 1.5 fault lengths of the surface rupture. As shown in Fig. 1, there are 16 wells in all and 15 of them respond to this large earthquake, whereas one well (YY) has no response.

For the tidal analysis, we limit the dataset to high quality water well records with well-resolved tides (Table 1). (Note: Because the surface rupture extends 300 km, the epicentral distances in Fig. 1 for some northern wells exceeds 1.5 fault lengths for well, e.g., PL and JY). We only study the eight wells with large amplitude responses to tides (responses >0.45 mm per nanostrain) to ensure that the tidal signal is well-separated from the noise level (Fig. 2). Because the digital upgrade of the network was carried out over a long period, the beginning of the water level records and the continuity of the data are different at each well. As a result, there is no uniform time period with high quality data for all of the wells. For seven wells, the reported water level is the distance between the wellhead and the water surface inside the well; for the one artesian well (ZZ), because the hydraulic head is higher than the ground, it is measured with a pressure transducer sampling inside a tube above the ground surface. We also check the timing of each well and make clock corrections as necessary based on the initial response time of the water level to the Wenchuan earthquake (Table 1).

3. Comparison of water level steps and static stress changes

Zhang and Huang (2011) and Shi et al. (2012) previously measured the coseismic water level changes, and used them to estimate the static poroelastic strain caused by the Wenchuan earthquake. By comparing the calculated strain to the theoretical strain from the Okada dislocation model, they concluded that within 500 km, the sign of the coseismic water level changes can effectively match the dislocation model, although the magnitudes may be hard to predict for some wells. The predicted values based on the Okada model are for homogeneous and isotropic media. However, the actual complex geology as well as the confinement of the aquifer can affect the magnitude to a large extent. Zhang and Huang (2011) attributed the magnitude difference to different Skempton's coefficients which are defined under undrained conditions.

Shi et al. (2012) studied seventeen nearfield wells with one-minute sampling interval data for eleven wells and hourly sampling for the remaining six wells. We do not have the hourly sampling data, but do have additional five wells from Gansu and Shaanxi Province with one-minute sampling. These new data fill in a gap in the previous dataset to the northeast of the mainshock rupture. As shown in Fig. 1b, the coseismic water level change pattern of twelve wells matches the overall pattern previously reported. The area to the East identified as extensional, has decreasing water levels whereas the regions identified as compressional along strike have increasing water levels. The water

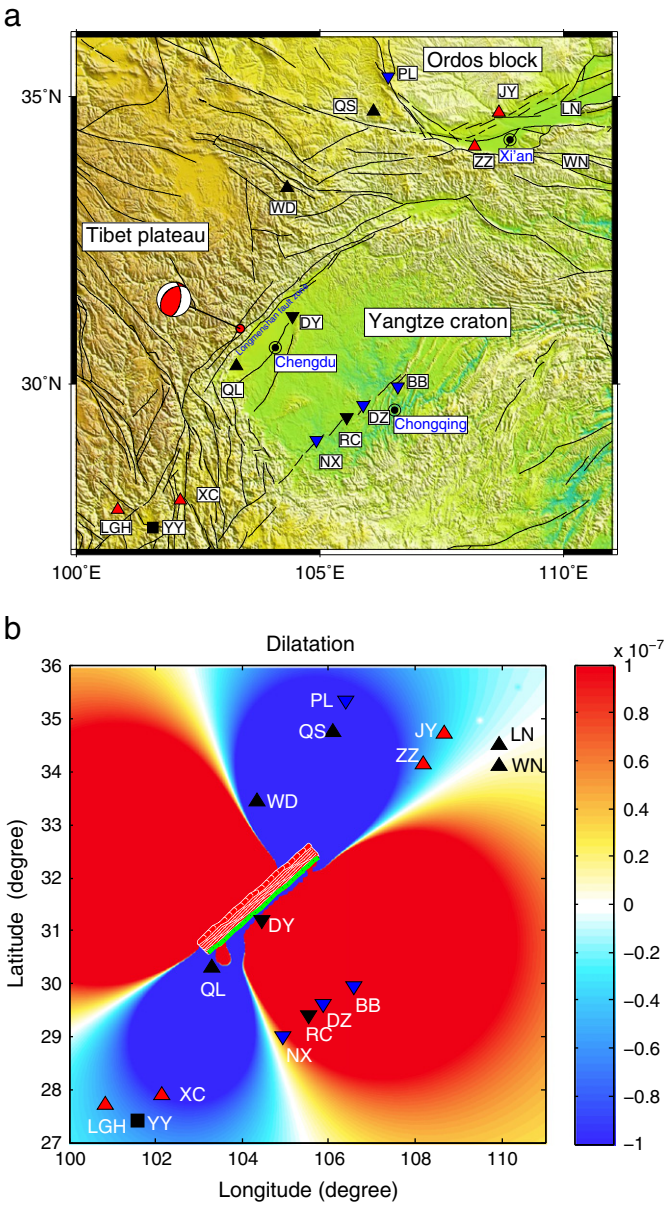

Fig. 1. (a) The epicenter location (red filled circle) of the M_w 7.9 Wenchuan earthquake on May 12, 2008 and the groundwater level observation wells within ~1.5 fault lengths. "Beach ball" shows the lower hemisphere projection of focal mechanism (strike 225°/dip 39°/rake 120°) of the earthquake (Zhang et al., 2009). Triangles imply coseismic water level rise and inverted triangles imply coseismic water level fall. The black square indicates no observed coseismic change in the well YY. The red triangles and blue inverted triangles indicate the wells we used for tidal analysis in this work. All capital letters (such as the WD, DY ect.) represent different well names. Black lines indicate the location of faults (Deng et al., 2004). The main cities (black circles), geological units and faults are shown in the map. (b) The calculated coseismic poroelastic strain (Lin and Stein, 2004; Toda et al., 2005) based on the finite fault model of Chen Ji (http://www.geol.ucsb.edu/faculty/ji/big_earthquakes/2008/05/12/ShiChuan.html), positive for dilatation, as well as the coseismic water level change pattern for the 16 wells. The meanings of the triangles, inverted triangles, square and capital letters are the same to (a).

Table 1
Basic information about the eight wells that have resolvable tidal responses, as well as the theoretical and actual initial response times of the water level to the M_w 7.9 Wenchuan earthquake that happened on May 12, 2008 at 14:28 local time. We assume the initial response is coincident with the P-waves, calculate the travel times for the P wave by the IASP91 model (Kennett and Engdahl, 1991), and make clock corrections as necessary.

Well	Aquifer lithology	Ground water flow type	Well depth (m)	Open interval (m)	Epicentral distance (km)	Theoretical response time	Actual response time	Clock correction (min)
DZ [a]	Mudstone/sandstone	fracture	109	45.5–109	286.13	14:29	14:31	2
NX [b]	sandstone	fracture	102	57.5–102	268.62	14:29	14:25	−4
BB [a]	sandstone	fracture	105	42.1–105	330.82	14:29	14:31	2
PL[c]	sandstone	pore	617	96.8–617	559.55	14:30	14:29	−1
XC [b]	gabbro	fracture	766	105.0–766	363.24	14:30	14:31	1
LGH[d]	limestone	fracture	200	102–106.7 122.1–133.6 179.3–183.7	437.20	14:30	14:30	0
JY [e]	limestone	fracture	495	95.5–495	647.78	14:30	14:32	2
ZZ [f*]	sandstone	pore	2778	2341–2658	572.11	14:30	14:32	2

*Well ZZ is an artesian well.
Basic information about the wells:
[a] : provided by H. -M. Wei working in Chongqing Earthquake Administration;
[b] : Sichuan Earthquake Administration (2004);
[c] : Gansu Earthquake Administration (2005);
[d] : Gong (2009);
[e] : provided by X. -L. Yang working in Shaanxi Earthquake Administration;
[f] : Shaanxi Earthquake Administration (2005).

level at well YY did not respond to this large earthquake, and we cannot see any tidal responses at the frequency of M_2 and O_1 wave for this well (see below), thus we speculate that this well-aquifer may be poorly confined with significant water table drainage. The well LN and WN are located near the nodal plane; although the predicted strain is quite small, coseismic steps are shown in the water levels. The well PL is located in the compressional area but shows coseismic decrease in water level, which may need further research.

Most of the wells show signs of coseismic water level changes tracking the poroelastic model, suggesting that the poroelastic response is dominant in determining the water level response in the nearfield. The match between the poroelastic strain and the water level responses is not new to this study, but is important to reconfirm with the current dataset as it will have important implications for the interpretation of the other measurements.

4. Tidal response method

The amplitude and phase responses of water level to Earth tides have been used to monitor aquifer storativity and permeability, respectively (Doan et al., 2006; Elkhoury et al., 2006; Hsieh et al., 1987; Xue et al., 2013). In a confined system, small phase lags result from high permeability whereas large phase lags result from low permeability. The amplitude response is primarily a measure of specific storage. The most commonly analyzed phase is M_2 because of its large amplitude and relatively low contamination by barometric pressure or diurnal temperature fluctuations (Doan et al., 2006; Hsieh et al., 1987; Rojstaczer and Agnew, 1989). In this work, we will also focus on the M_2 phase in our analysis.

We first calculated the tidal volumetric strain imposed by the solid Earth tides and ocean tides for each well by the "SPOTL" program (Agnew, 1997, 2012; Berger et al., 1987). We extract the tidal responses in the time domain by least squares fitting method as Hsieh et al. (1987) described. The water level h is expressed as:

$$h\left(t_j\right) = \sum_{k=1}^{N} a_k \cos\left(\omega_k t_j + \zeta_k\right) + e_j \tag{1}$$

and the dilatation strain ε is expressed as:

$$\varepsilon\left(t_j\right) = \sum_{k=1}^{N} A_k \cos\left(\omega_k t_j + \theta_k\right) + E_j \tag{2}$$

where t_j is the time of data point j; $h(t_j)$ and $\varepsilon(t_j)$ are the water level and dilatation strain at time t_j respectively; N the number of tidal constituents used in analysis, ω_k the frequency of the kth tidal constituent; a_k and ζ_k are the amplitude and phase angle of the kth tidal constituent in the water level; A_k and θ_k the amplitude and phase angle of the kth tidal constituent in the dilatation strain. e_j and E_j are the residual in water level and dilatation strain at data point j. The amplitude response is equal to a_k/A_k, and the phase shift is $\zeta_k - \theta_k$. In this work, O_1, K_1, M_2 and S_2 waves are simultaneously fit in the tidal analysis, and their periods are 1.0758, 0.9973. 0.5175 and 0.5000 days, respectively (Wilhelm et al., 1997). Only the strongest phase (M_2) is used for subsequent interpretation.

There are gaps in the original water level data that need preprocessing before tidal analysis. If the gap is less than 10 points (10 min), we interpolate linearly; if the gap is larger, we set the values to be zero. We demean and detrend the non-zero water level data, and then filter all the water level and synthetics from 10 h to 30 h by a 2 pass second-order Butterworth band-pass filter, so that only diurnal and semi-diurnal tidal components and some noise are left in this band. We further set the filtered water level data that are affected by edge effects to be zero and set the corresponding theoretical tides to be zero as well. Then we divided the data into different segments with each segment of 29.5 days, so that we can distinguish the M_2 wave from the S_2 wave. The segments are overlapped by 10% of the segment length. Then the least squares fitting procedure is applied to each segment. If the number of zero in one segment is more than 10% of the segment length, we will skip that segment. Otherwise we will plot the results at the center of each window. Finally we can obtain the tidal responses as a function of time for each well. The amplitude and phase responses of the eight wells are shown in Fig. 3. Amplitude response is the ratio of Earth tides to water level and the phase response is defined so that negative phases mean the water level lags behind the dilatational strain of the Earth tides, whereas positive phases mean the water level leads.

To study the permeability and storativity variations caused by the Wenchuan earthquake, we pick out the points within 30 days before the earthquake for each well, and estimate the mean value of these points as the initial amplitude and phase response. Then we calculate the mean value of the points within 30 days after the earthquake, and use it to subtract the initial value, so as to obtain the amplitude and phase change caused by the earthquake. For comparison, we also calculate the standard deviation of the phases and amplitudes before the earthquake for each well as the background variability. The results are shown in Table 2.

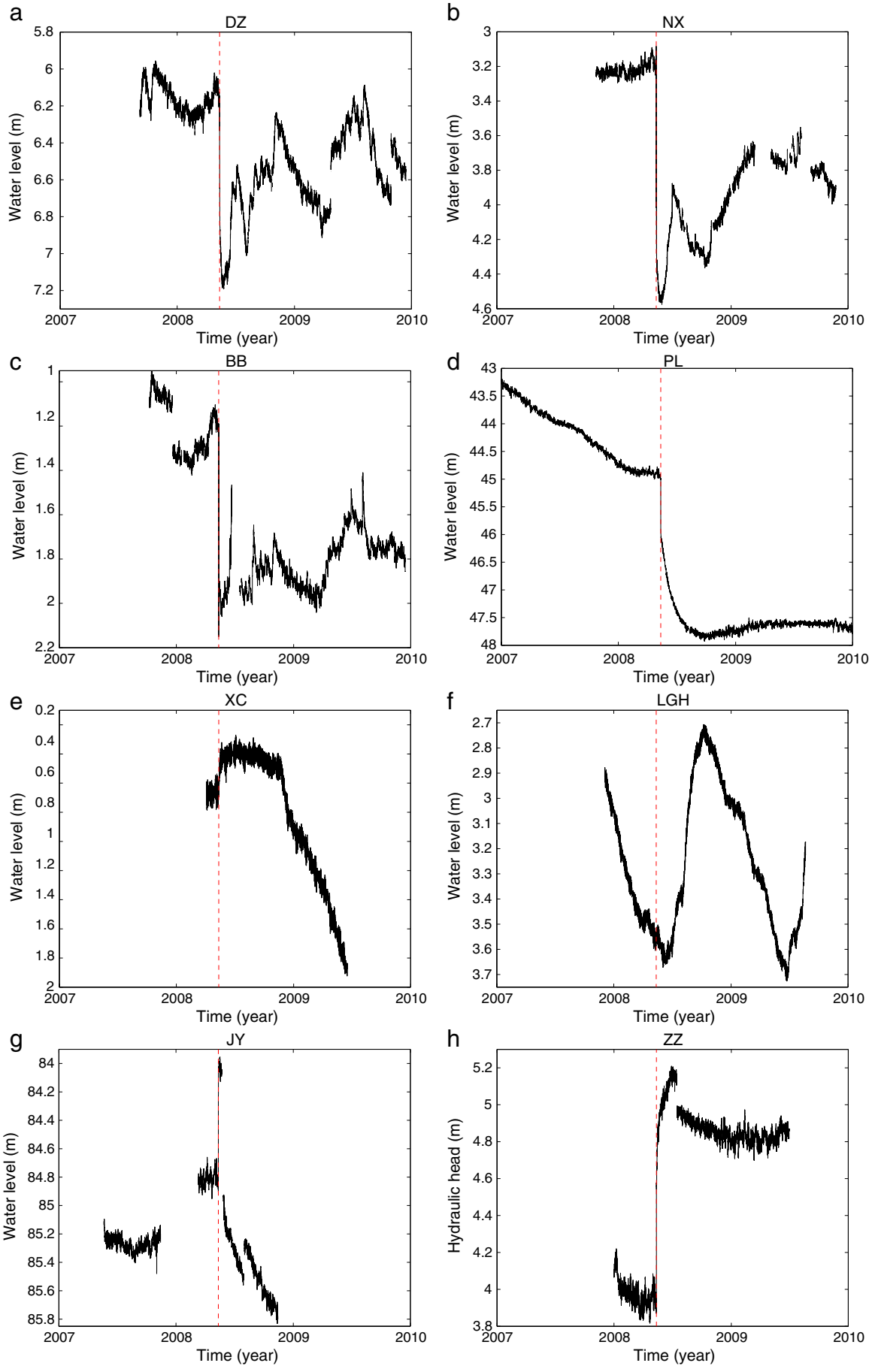
a
DZ
Water level (m)
Time (year)
b
NX
Water level (m)
Time (year)
c
BB
Water level (m)
Time (year)
d
PL
Water level (m)
Time (year)
e
XC
Water level (m)
Time (year)
f
LGH
Water level (m)
Time (year)
g
JY
Water level (m)
Time (year)
h
ZZ
Hydraulic head (m)
Time (year)

5. Tidal response observations

5.1. Permeability enhancement in the nearfield

The tidal responses over time for the eight wells are shown in Fig. 3. Both phase leads and phase lags are observed. The phases are always negative for wells DZ, PL and XC and positive for wells BB and JY. For the well LGH, phases are negative before the earthquake and become positive after the earthquake. For the wells ZZ and NX, the phases are around zero before the earthquake and become positive after the earthquake.

According to Hsieh et al. (1987), for a single, homogeneous, isotropic, laterally extensive and confined aquifer, the phase shifts between Earth tides and water level are assumed to be caused by the time required for water flowing into and out of the well; in that case, the water table drainage effect is ignored and the phase shifts should be always negative, and phase shift increase (such as from −5° to −1°) implies transmissivity or permeability increase (Elkhoury et al., 2006; Hsieh et al., 1987). In this work, however, positive phase shifts are commonly observed (Fig. 3), indicating the model of Hsieh et al. (1987) is not enough to describe the response of water level to Earth tides for this dataset.

Roeloffs (1996) presented a model in which the vertical drainage to the water table can cause positive phase shifts. As shown in Fig. 4, the phase lead of water level relative to Earth tides is observable directly in the raw data and not due to cycle skipping. The apparent lack of causality (phase lead) is a result of translating the solution of a diffusion equation in terms of mass increment to a resultant pore pressure (Wang, 2000, Section 6.9). As pointed out by Roeloffs (1996), all aquifers respond as confined systems to very short-period disturbances, and drain to the water table in response to sufficiently long-period disturbances. At the tidal period (12.42 h for M_2) a combination of effects is possible (partial confinement).

In our dataset, wells ZZ, NX and LGH all change the sign of the phase over time (Fig. 3). Therefore, neither end-member model is viable. The observed phase shift is a combination of the phase lag due to borehole storage effect and the phase lead due to water table drainage. If we want to precisely quantify the permeability variation with time, we have to separate the two effects. This could be done with two closely spaced wells sampling vertically offset intervals, but cannot be done with the current data.

Although we are hindered by this problem, both in the horizontal fluid flow model (Hsieh et al., 1987) and in the vertical pore pressure diffusion model (Roeloffs, 1996), the observed phase responses can be considered as a measurement of permeability, and phase shift increase (such as from 5° to 10°) implies permeability increase. Therefore, we only report the relative changes in phase and the associated sign of the permeability changes to ensure that the results are robust regardless of the degree of water table drainage at the tidal periods.

As shown in Table 2, for six wells the coseismic phase shift increases and the amplitude of the increase is greater than the background phase variability. These increases in phase imply that the permeability increases at these wells after the Wenchuan earthquake. For wells PL and XC, the coseismic phase change is less than the background variability and therefore insignificant. For the well LGH, phase shift increases about 17.4° from negative to positive, implying vertical flow may be dominant for this well after the earthquake. As previously noted, the coseismic water level change pattern in the region of the large M_w 7.9 Wenchuan earthquake mainly tracks the static poroelastic strain (Shi et al., 2012; Zhang and Huang, 2011); here the permeability increases at most of the wells regardless of whether the coseismic response for the well water level is increasing or decreasing, implying permeability enhancement is a distinct process from static poroelastic strain. A more complex, multistage process such as fracture formation or unclogging is required (Brodsky et al., 2003; Elkhoury et al., 2006; Manga et al., 2012).

5.2. Permeability recovery time after the earthquake

For many of the wells the permeability change is not permanent. The phase response decays gradually towards the original value, as shown in Fig. 3. Because of the noise, we cannot tell the recovery time for three wells; however, for the other five wells, we can see the recovery time for the wells DZ, NX and BB are six to ten months; for the wells LGH and JY, it does not recover at 460 days and 180 days. It seems that the recovery time may be shorter for the wells located in the basin whose well depths are quite shallow and longer (some did not recover) for the wells located in the mountain whose well depths are deeper. We speculate that there may be more fine grains in the basin that are prone to re-clog the flow channel. Besides, the aquifer lithology for the wells LGH and JY is limestone, from which it may be more difficult to produce grains to re-clog the flow channel than sandstone and mudstone. As the coseismic phase shift increases 17.4° for the well LGH, it is also possible that new fractures may be formed. We noticed that after a period of time, the permeability for the well DZ is lower than the pre-seismic level. This may be because the aquifer lithology is mainly mudstone. The barriers were vibrated by the seismic waves during the earthquake, then they deposited gradually and may gather tightly and block part of the fractures that were open before the earthquake.

Manga et al. (2012) has compiled the time to permeability recovery from recent studies based on different types of observation, such as the groundwater level, springs, streamflow, groundwater chemistry and water injection, and the recovery time scales are from minutes (exponential decay time) to several years. The results here are compatible with most observations with the exception of Geballe et al. (2011). Investigating the physical origin of the distinction may be a useful subject for future research.

6. Conclusions

We observe a systematic phase shift increase of the tidal response at most stations near the Wenchuan earthquake, regardless of the orientation of the poroelastic strain. This observation shows that dynamic permeability enhancement happens in the nearfield, simultaneously with the coseismic water level changes that have been previously attributed to static stress changes.

Acknowledgments

This work made use of GMT and MATLAB software. The groundwater level data are from the Groundwater Monitoring Network of China Earthquake Networks Center. Many thanks to Duncan C. Agnew for providing the "SPOTL" program for calculating the tidal volumetric strain, and thank Kuo-Fong Ma, Patrick Fulton and the two reviewers for their instructive suggestions. This work was supported by the Wenchuan earthquake Fault Scientific Drilling project, National Natural Science Foundation of China with Grant No.41174040 and No. 41274061, NSF EAR-1045825 and China Scholarship Council.

Fig. 2. Water level records for the eight wells that have resolvable tidal responses. The start time and end time of the data for each well are not uniform. Among the eight wells, only the well ZZ is an artesian well and hydraulic head is measured in this well. For the other seven wells, the water level is the distance between the wellhead and the water surface inside the well. The red dotted lines indicate the start time of the M_w 7.9 Wenchuan earthquake at 14:28 on May 12, 2008 (Beijing time); the coseismic water level changes are significant at each well.

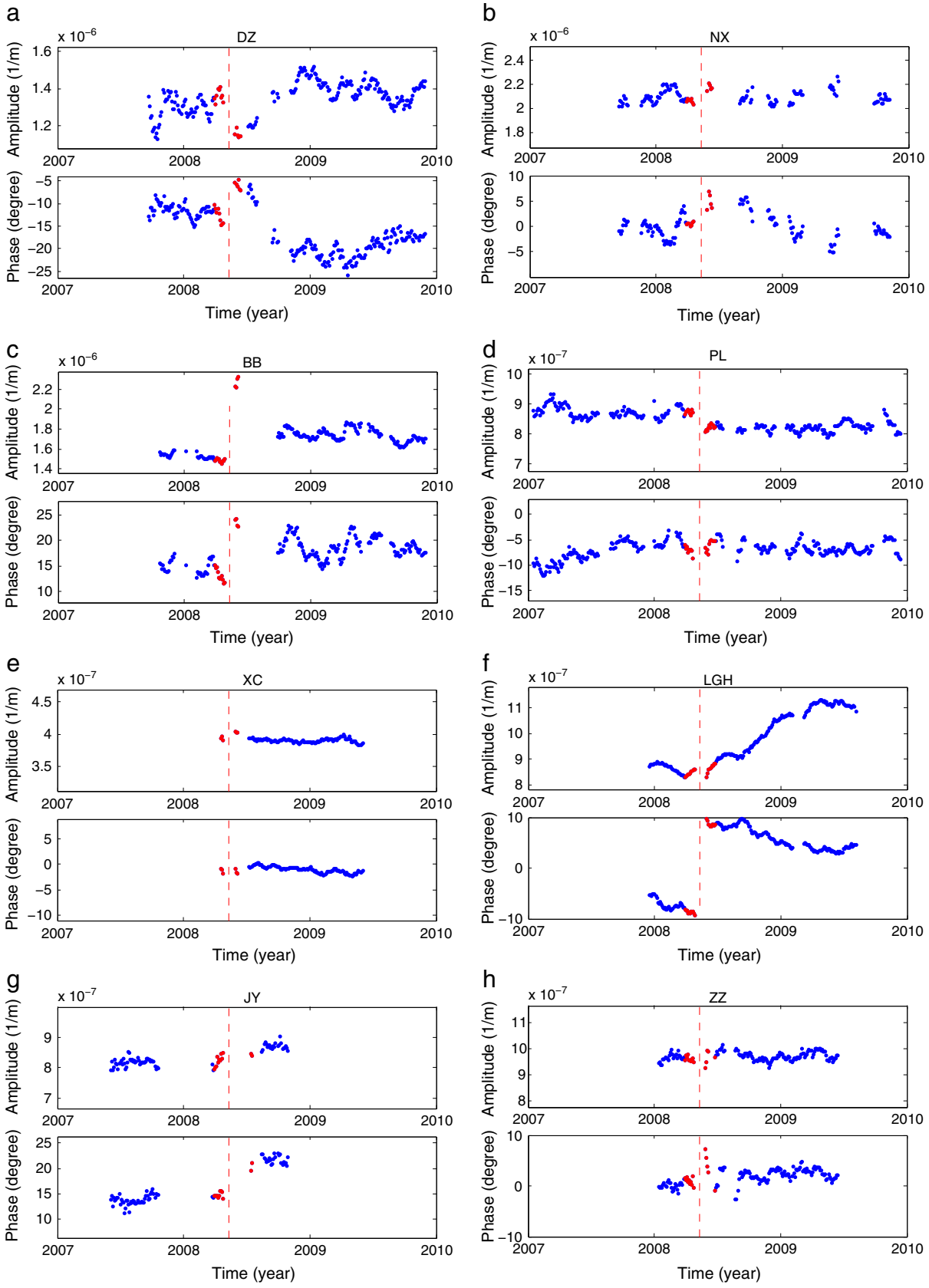

Fig. 3. Amplitude and phase responses over time for the eight wells at the frequency of M_2 wave. The amplitude response is the amplitude ratio of Earth tides over water level. The start time and end time of the data for the wells are not uniform. The red dotted lines show the start time of the M_w 7.9 Wenchuan earthquake on May 12, 2008 at 14:28 (Beijing time). The red dots show the amplitude and phase response within 30 days before and after the earthquake. For the well JY, there are no values within 30 days after the earthquake; we selected the points within 60 days after the earthquake instead. Except for the well PL and XC, the phase shifts at the other six wells increased obviously after the earthquake, and the amplitude responses also changed for most of the wells.

Table 2
The coseismic water level changes, phase and amplitude response and the recovery time for the eight wells. The reported initial phases and amplitudes are the average value of the points within 30 days before the earthquake. The background phase and amplitude variability are the standard deviation of the phases and amplitudes before the earthquake for each well. The reported phase and amplitude change are obtained by the average value of the points within 30 days after the earthquake minus the initial phase and amplitude. Recovery times are approximated from inspection of Fig. 3a–c,f–g and "N/A" means the recovery times are not clear due to the background noise.

Well	Coseimic response	Initial phase (°)	Background phase variability (°)	Coseismic phase change (°)	Initial amplitude($\times 10^{-6}$ 1/m)	Background amplitude variability($\times 10^{-6}$ 1/m)	Coseismic amplitude change($\times 10^{-6}$ 1/m)	Positive phase	Approximate Recovery time (day)
DZ	down	−13.7	1.5	6.7	1.36	0.06	−0.21	No	~200
NX	down	0.5	1.8	4.3	2.06	0.05	0.11	Yes	~300
BB	down	13.2	1.5	10.3	1.49	0.03	0.78	Yes	~300
PL	down	−7.0	2.1	1.0	0.87	0.02	−0.05	No	N/A
XC	up	−1.3	0.5	−0.1	0.39	0.003	0.01	No	N/A
LGH	up	−8.7	1.1	17.4	0.85	0.02	0.02	After event	Not recovered at 460
JY[a]	up	14.8	1.0	5.5	0.82	0.01	0.02	Yes	Not recovered at 180
ZZ	up	0.93	0.8	2.7	0.96	0.004	0.004	Yes	N/A

[a] For the well JY, there are no values within 30 days after the earthquake; we selected the points within 60 days after the earthquake instead.

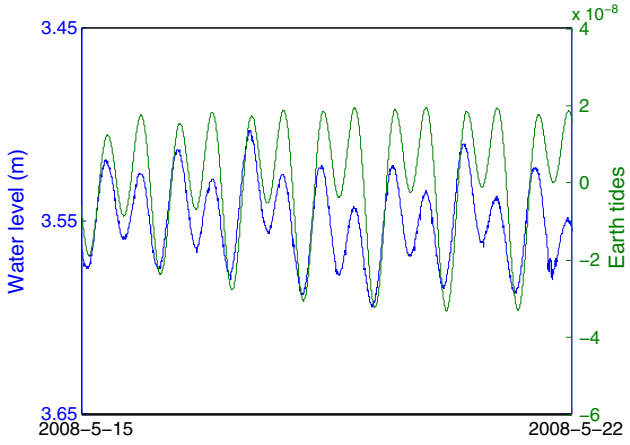

Fig. 4. The recorded water level and calculated Earth tides for well LGH after the Wenchuan earthquake. The phase lead of water level relative to Earth tides is observable directly in the raw data and not due to cycle skipping.

References

Agnew, D.C., 1997. NLOADF: a program for computing ocean-tide loading. J. Geophys. Res. 102, 5109–5110.

Agnew, D.C., 2012. SPOTL: some programs for ocean-tides loading. Technical Report. Scripps Institution of Oceanography, La Jolla, CA.

Akita, F., Matsumoto, N., 2001. Coseismic groundwater level changes in hot spring wells in Hokkaido induced by four earthquakes larger than M7. 5 between 1993 and 1994. Jishin. J. Seismol. Soc. Jpn. 53 (3), 193–204.

Akita, F., Matsumoto, N., 2004. Hydrological responses induced by the Tokachi-oki earthquake in 2003 at hot spring wells in Hokkaido, Japan. Geophys. Res. Lett. 31 (16), L16603.

Berger, J., Farrell, W., Harrison, J.C., Levine, J., Agnew, D.C., 1987. ERTID 1: A Program for Calculation of Solid Earth Tides. Publication of the Scripps Institution of Oceanography, La Jolla, CA.

Brodsky, E.E., Roeloffs, E.A., Woodcock, D., Gall, I., Manga, M., 2003. A mechanism for sustained groundwater pressure changes induced by distant earthquakes. J. Geophys. Res. 108 (B8), 2390. http://dx.doi.org/10.1029/2002JB002321.

Chia, Y., Chiu, J.J., Chiang, Y., Lee, T., Liu, C., 2008. Spatial and temporal changes of groundwater level induced by thrust faulting. Pure Appl. Geophys. 165 (1), 5–16.

Deng, Q.-D., Zhang, P.-Z., Ran, Y.-K., 2004. Distribution of Active Faults in China (1:4000000). Science Press, Beijing.

Doan, M.L., Brodsky, E.E., Prioul, R., Signer, C., 2006. Tidal analysis of borhole pressure — a tutorial. Schlumberger Research Report.

Elkhoury, J.E., Brodsky, E.E., Agnew, D.C., 2006. Seismic waves increase permeability. Nature 441 (7097), 1135–1138.

Gansu Earthquake Administration, 2005. Seismic Monitoring Record of Gansu province. Lanzhou University Press, Lanzhou 127–129 (in Chinese).

Geballe, Z.M., Wang, C.-Y., Manga, M., 2011. A permeability-change model for water-level changes triggered by teleseismic waves. Geofluids 11 (3), 302–308.

Gong, H.-B., 2009. The research of groundwater level micro-dynamic responding to stress. Jilin University 38–39 (M.D. thesis, (in Chinese)).

Hsieh, P.A., Bredehoeft, J.D., Farr, J.M., 1987. Determination of aquifer transmissivity from earth tide analysis. Water Resour. Res. 23 (10), 1824–1832.

Huang, F.-Q., 2008. Response of well in groundwater monitoring network in Chinese mainland to distant large earthquakes. Institute of Geophysics, China Earthquake Administration (Ph.D. dissertation (in Chinese)).

Huang, F.-Q., Jian, C.-L., Tang, Y., Xu, G.-M., Deng, Z.-H., Chi, G.-C., 2004. Response changes of some wells in the mainland subsurface fluid monitoring network of China, due to the September 21, 1999, Ms7. 6 Chi-Chi Earthquake. Tectonophysics 390 (1), 217–234.

Kennett, B.L.N., Engdahl, E.R., 1991. Traveltimes for global earthquake location and phase identification. Geophys. J. Int. 105 (2), 429–465.

Lee, T.-P., Chia, Y., Yang, H., Liu, C., Chiu, Y., 2012. Groundwater level changes in Taiwan caused by The Wenchuan earthquake on 12 May 2008. Pure Appl. Geophys. 169 (11), 1947–1962.

Lee, S.H., Ha, K., Hamm, S.Y., Ko, K.S., 2012. Groundwater responses to the 2011 Tohoku Earthquake on Jeju Island, Korea. Hydrol. Process 27 (8), 1147–1157. http://dx.doi.org/10.1002/hyp.9287.

Lin, J., Stein, R.S., 2004. Stress triggering in thrust and subduction earthquakes and stress interaction between the southern San Andreas and nearby thrust and strike slip faults. J. Geophys. Res. 109, B02303.

Liu, L.-B., Roeloffs, E.A., Zheng, X.-Y., 1989. Seismically induced water level fluctuations in the Wali well, Beijing, China. J. Geophys. Res. 94 (B7), 9453–9462.

Manga, M., 2001. Origin of postseismic streamflow changes inferred from baseflow recession and magnitude–distance relations. Geophys. Res. Lett. 28 (10), 2133–2136.

Manga, M., Rowland, J.C., 2009. Response of Alum Rock springs to the October 30, 2007 Alum Rock earthquake and implications for the origin of increased discharge after earthquakes. Geofluids 9 (3), 237–250.

Manga, M., Brodsky, E.E., Boone, M., 2003. Response of streamflow to multiple earthquakes. Geophys. Res. Lett. 30 (5), 1214.

Manga, M., Beresnev, I., Brodsky, E.E., Elkhoury, J.E., Elsworth, D., Ingebritsen, S.E., David, C.M., Wang, C.-Y., 2012. Changes in permeability caused by transient stresses: field observations, experiments, and mechanisms. Rev. Geophys. 50 (2), RG2004. http://dx.doi.org/10.1029/2011RG000382.

Matsumoto, N., Roeloffs, E.A., 2003. Hydrological response to earthquakes in the Haibara well, central Japan — II. Possible mechanism inferred from timevarying hydraulic properties. Geophys. Res. Lett. 155 (3), 899–913.

Mohr, C.H., Montgomery, D.R., Huber, A., Bronstert, A., Iroume, A., 2012. Streamflow response in small upland catchments in the Chilean coastal range to the MW 8.8 Maule earthquake on 27 February 2010. J. Geophys. Res. Earth Surf. 117, F02032.

Montgomery, D.R., Manga, M., 2003. Streamflow and water well responses to earthquakes. Science 300 (5628), 2047–2049.

Niwa, M., Takeuchi, R., Onoe, H., Tsuyuguchi, K., Asamori, K., Umeda, K., Sugihara, K., 2012. Groundwater pressure changes in Central Japan induced by the 2011 off the Pacific coast of Tohoku Earthquake. Geochem. Geophys. Geosyst. 13 (5), Q05020.

Roeloffs, E.A., 1996. Poroelastic techniques in the study of earthquake-related hydrologic phenomena. Adv. Geophys. 37, 135–195.

Roeloffs, E.A., Bredehoeft, J.D., 1985. Coseismic response of water wells near Parkfield, California, to the August 4, 1985 Kettleman Hill earthquake. EOS Trans. Am. Geophys. Union 66, 986.

Rojstaczer, S., Agnew, D.C., 1989. The influence of formation material properties on the response of water levels in wells to Earth tides and atmospheric loading. J. Geophys. Res. 94 (B9), 12403–12411.

Shaanxi Earthquake Administration, 2005. Seismic Monitoring Record of Shaanxi Province. Seismological Press, Beijing 68–71 (in Chinese).

Shi, Z.-M., Wang, G.-C., Liu, C.-L., 2012. Co-seismic groundwater level changes induced by the May 12, 2008 Wenchuan Earthquake in the Near Field. Pure Appl. Geophys. http://dx.doi.org/10.1007/s00024-012-0606-1 (in press).

Shibata, T., Matsumoto, N., Akita, F., Okazaki, N., Takahashi, H., Ikeda, R., 2010. Linear poroelasticity of groundwater levels from observational records at wells in Hokkaido, Japan. Tectonophysics 483 (3), 305–309.

Sichuan Earthquake Administration, 2004. Seismic monitoring record of Sichuan province. Chengdu Map Press, Chengdu 381–383 (397–400 (in Chinese)).

Sil, S., 2006. Response of Alaskan wells to near and distant large earthquakes. University of Alaska Fairbanks (M. D. thesis).

The Monitoring and Forecasting Department of China Earthquake Administration, 2007. Theoretical basis and observation techniques of seismic underground fluids. Seismological Press, Beijing.

Toda, S., Stein, R.S., Richards-Dinger, K., Bozkurt, S., 2005. Forecasting the evolution of seismicity in southern California: animations built on earthquake stress transfer. J. Geophys. Res. 110, B05S16.

Wakita, H., 1975. Water wells as possible indicators of tectonic strain. Science 189 (4202), 553.
Wang, H.F., 2000. Theory of linear poroelasticity with applications to geomechanics and hydrogeology. Princeton University Press, New Jersey 136–138.
Wang, C.-Y., Chia, Y., 2008. Mechanism of water level changes during earthquakes: near field versus intermediate field. Geophys. Res. Lett. 35 (12), L12402.
Wang, C.-Y., Manga, M., Dreger, D., Wong, A., 2004. Streamflow increase due to rupturing of hydrothermal reservoirs: evidence from the 2003 San Simeon, California, earthquake. Geophys. Res. Lett. 31 (10), L10502.
Wang, C.-Y., Chia, Y., Wang, P.-L., Dreger, D., 2009. Role of S waves and Love waves in coseismic permeability enhancement. Geophys. Res. Lett. 36 (9), L09404.
Wilhelm, H., Zurn, W., Wenzel, H.-G. (Eds.), 1997. Tidal Phenomena, volume 66 of Lecture Notes in Earth Sciences. Springer, Berlin, Germany, p. 22.
Xue, L., Li, H.-B., Brodsky, E.E., Xu, Z.-Q., Kano, Y., Wang, H., Mori, J.J., Si, J.-L., Pei, J.-L., Zhang, W., Yang, G., Sun, Z.-M., Huang, Y., 2013. Continuous permeability measurements record healing inside the Wenchuan Earthquake Fault Zone. Science 340 (6140), 1555–1559. http://dx.doi.org/10.1126/science.1237237.
Yang, Z.-Z., Deng, Z.-H., Liu, C.-G., Wang, G.-Q., Zu, J.-H., Tao, J.-L., Song, J., 2008. Co-seismic changes of water level and water temperature caused by MS 8.0 Wenchuan earthquake. Seismol. Geol. 30 (4), 895–905 (in Chinese).
Zhang, Y., Huang, F.-Q., 2011. Mechanism of different coseismic water-level changes in wells with similar epicentral distances of intermediate field. Bull. Seismol. Soc. Am. 101 (4), 1531–1541.
Zhang, Y., Feng, W.-P., Xu, L.-S., Zhou, C.-H., Chen, Y.-T., 2009. Spatio-temporal rupture process of the 2008 great Wenchuan earthquake. Sci. China Ser. D 52 (2), 145–154.